

# Values of the ozone entrainment flux for the one-box photochemical model

S.A. Rumyantsev and V.C. Roldugin

*Polar Geophysical Institute, Kola Scientific Center of the Russian Academy of Sciences, Apatity, Murmansk Region*

Received April 7, 2004

We consider the behavior of numerical solutions obtained using simple photochemical model of the surface atmosphere that assumes uniform distribution of the components over the mixing layer. The mean ozone entrainment flux from above into the mixing layer is determined. These entrainment flux values are required for reaching the equality between the average ozone concentrations in the beginning of the calculated diurnal period and in its end. The diurnal variation of the surface ozone experimentally observed at the high-latitude observatory in Lovozero (Murmansk Region) is discussed and it is shown that the average surface ozone concentrations at 0 a.m. and 24 p.m. (local time) are equal to each other within the accuracy of tenths of ppb. Comparison is made of the calculated ozone entrainment flux with the experimental data on the ozone flux from the stratosphere to the troposphere at the tropopause in different seasons. It has been found that if the total value of the ozone entrainment flux at mid-latitudes is equal approximately to  $5 \cdot 10^{10} - 1.2 \cdot 10^{11} \text{ cm}^{-2} \cdot \text{s}^{-1}$ , then at high latitudes this value is assumed to be considerably higher in the model discussed here.

## Introduction

Chemically, ozone is one of the most active minor components of the Earth's atmosphere.<sup>1</sup> High chemical activity of the ozone causes its strong destructive impact on different materials and biological objects. It is a contaminant of the atmosphere reducing the air quality.<sup>2</sup> The presence of ozone in large quantities may cause deterioration of the human health. Ozone is one of the important greenhouse gases.

Ozone is mainly produced in the stratosphere due to the dissociation of molecular oxygen under the impact of short-wave solar ultraviolet radiation (UVR). A part of the stratospheric ozone amount penetrates from the stratosphere into the troposphere, thus partly forming the ozone flux absorbed in the troposphere and on the Earth's surface. Another one part of the tropospheric ozone flux is generated in the troposphere under the action of long-wave portion of the solar ultraviolet radiation. Both parts form the ozone entrainment flux at the upper boundary of the mixing layer. These components of the flux correspond to two sources of the tropospheric ozone: transfer from the stratosphere and the local generation by the solar ultraviolet generation. Both sources have comparable powers.<sup>3</sup> As was shown experimentally<sup>3</sup> in summer in the northern part of Canada the photochemical processes yield the main contribution to the ozone content in the atmospheric boundary layer; the second important source here is the transfer from the upper atmosphere.

The tropospheric ozone flux is equal to the sum of the ozone flux from the stratosphere at the tropopause altitude (at the upper boundary of the troposphere) and the ozone entrainment flux at the

upper boundary of the mixing layer. The ozone flux value through the tropopause is known from measurements<sup>3,4</sup> as are the values of the ozone flux on the Earth's surface,<sup>5,6</sup> while the values of the ozone entrainment flux have not been found experimentally. To determine the values of the ozone entrainment flux, different theoretical assumptions<sup>7</sup> are used. In this paper the values of the ozone entrainment flux in the mixing layer were calculated from the characteristics of the solution of a photochemical model and characteristics of the ozone distribution observed.

## The model

To solve this problem, we use a simple one-box photochemical model.<sup>8</sup> In this case we assume that in a certain atmospheric layer adjacent to the surface (the mixing layer<sup>9</sup>), the minor gases are distributed uniformly over height. In this idealized case the concentration of a gaseous contaminant is assumed constant in the mixing layer.<sup>9</sup> This assumption is quite realistic for volatile organic compounds (VOC), for which the relative homogeneity of their distribution over the mixing layer was observed experimentally.<sup>10</sup> In the model used the distribution of all gaseous contaminants in the mixing layer is taken to be constant with height. This model describes quite well a number of the basic characteristics of ozone distribution under the background conditions as well as in the contaminated areas.<sup>11</sup>

Characteristics of the model are given in detail in Ref. 8. The model describes the chemical transformation of 9 gases:  $\text{O}_3$ ,  $\text{NO}$ ,  $\text{NO}_2$ ,  $\text{NO}_3$ ,  $\text{N}_2\text{O}_5$ ,  $\text{HNO}_3$ ,  $\text{CH}_2\text{O}_3$ , peroxyacetylnitrate, and  $\text{HO}_2$  in the mixing layer where the concentrations of these

components are assumed independent of height. These components react with one another and with the solar ultraviolet radiation through 30 reactions, presenting basic interactions in the atmospheric boundary layer and including 3 reactions of photodissociation of  $\text{NO}_2$  and  $\text{NO}_3$ . The list of these reactions can be found in Ref. 8; the reaction rates are taken from Ref. 12 and 13; the rate of interaction of NO with organic peroxide radicals  $\text{RO}_2$  was taken from Ref. 14. It is assumed that the atomic oxygen, being produced, is immediately transformed into the ozone. The following compounds were taken into account as predetermined: molecular hydrogen, water vapor, hydroxyl, carbon monoxide, formaldehyde, methane, and organic peroxy radicals  $\text{RO}_2$ .

Using the model, we have found the solution of equations of chemical kinetics with the account of dry deposition

$$dn(i)/dt = S_i - L_i - v(i)n(i)/h, \quad (1)$$

where  $n(i)$  is the concentration of the  $i$ th component,  $i = 1, 2, \dots, 9$ ;  $S_i$ ;  $L_i$  are the terms describing sources and sinks of the  $i$ th component, respectively;  $v_i$  denotes the rates of dry deposition;  $h$  is the height of the mixing layer.

The source of the ozone  $S(\text{O}_3)$  includes both the term  $S_c(\text{O}_3)$  describing the ozone yield from chemical reactions, and the term  $S_t(\text{O}_3)$  specifies the ozone influx from the upper layers:  $S(\text{O}_3) = S_c(\text{O}_3) + S_t(\text{O}_3)$ . By the same procedure the source  $S(\text{NO})$  for nitric oxide includes the term  $S_c(\text{NO})$ , caused by chemical transmutations, and the term  $S_t(\text{NO})$  denoting the NO influx from the lower boundary of the mixing layer both as a result of biogenetic and anthropogenic activities. Sources  $S_t$  of the other components of the gas mixture are taken to be equal to zero for the simplicity of the problem. The value of the source function for ozone  $S_t = F/h$ , where  $F$  is the ozone entrainment flux at the upper boundary of the mixing layer by analogy to that given in Ref. 7.

The photodissociation rates of  $\text{NO}_2$ ,  $\text{NO}_3$ , concentrations of OH hydroxyl, and important precursors of ozone-organic peroxyradicals  $\text{RO}_2$  are given as the functions of local time – a positive branch of sinusoid in a period of solar irradiation of the atmosphere with the peak at noon, and are zero when the sun is beyond the horizon. In the solar irradiation period the main amount of the volatile organic compounds (VOC) is injected and the hydroxyl is generated, in reactions of which with VOC the organic peroxy radicals are produced.<sup>15–17</sup> Values of the hydroxyl concentration maxima were determined from the parameterization given in Ref. 18. The rates of dry deposition were taken from the literature and were independent of local time. For ozone the results from Ref. 19 for Alaska were used with the values of  $v(\text{O}_3) = 0.007$  m/s for summer and fall,  $v(\text{O}_3) = 0.0005$  m/s for winter; for spring we used the value of  $v(\text{O}_3) = 0.004$  m/s.<sup>20</sup> For the remaining gases the following values were taken:  $v(\text{NO}_2) = 0.003$  m/s,<sup>1</sup>  $v(\text{NO}_3) = v(\text{N}_2\text{O}_5) = v(\text{HNO}_3) =$

$$= v(\text{CH}_3\text{O}_2) = 0.2 \text{ m/s},^{21} \quad v(\text{PAN}) = 0.0026 \text{ m/s}.^{22}$$

The rate of dry deposition of NO is taken to be zero.

The intensity of ultraviolet radiation comes into the Eqs. (1) through the photodissociation rates. The behavior of the model at different levels of ultraviolet radiation was studied in Ref. 11. For the photodissociation rate of nitrogen peroxide in different seasons the values about  $5 \cdot 10^{-3} \text{ s}^{-1}$  were used as measured on Spitsbergen.<sup>23</sup>

Equations of chemical kinetics (1) were solved by Gear method of variable order with a variable step for rigid systems.

## Calculated results and discussion

One of the results of applying this model is diurnal behavior of the ozone and nitrogen oxides found. An example of the diurnal behavior of concentrations of these compounds is shown in Fig. 1 for summer of a northern region. In Fig. 1 the following values were used: the mean air temperature  $T = 15^\circ\text{C}$ ; the relative humidity 80%, the peak photodissociation rate of  $\text{NO}_2$  is  $4.2 \cdot 10^{-3} \text{ s}^{-1}$ , the sunshine duration was 22 hours, the maximum concentration of  $\text{RO}_2$  was  $3 \cdot 10^{-2}$  ppb (for  $\text{RO}_2$  we used the results of numerical simulation of the formation of organic peroxy radicals in the forest,<sup>17</sup> the growth rate of the NO concentration –  $S_t(\text{NO}) = 1.5 \cdot 10^{-5}$  ppb/s, the ozone entrainment flux  $F_1 = h \cdot S_t(\text{O}_3) = 2.84 \cdot 10^{11}$  molecules  $\text{O}_3/(\text{cm}^2 \cdot \text{s})$ . As the initial values the following ones were taken:  $n_0(\text{O}_3) = 30$  ppb,  $n_0(\text{NO}) = 0$ ,  $n_0(\text{NO}_2) = 1$  ppb, the mean height of the mixing layer  $h = 500$  m (based on the observation results given in Ref. 24).

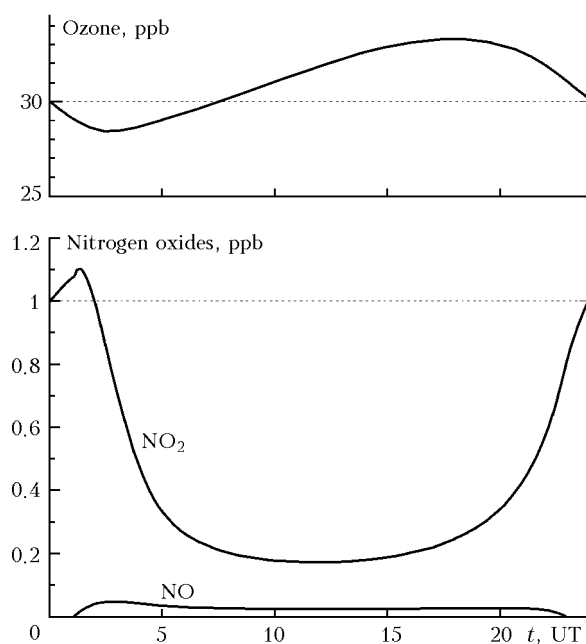


Fig. 1. Dependence of the ozone concentration and nitric oxides on time according to calculated results.

Figure 1 shows the process of photodissociation of nitrogen peroxide by the solar ultraviolet radiation and formed, in this case, atomic oxygen transforms into the ozone, and the nitric oxide, occurring in the course of photodissociation, interacts with the ozone precursors and forms the nitrogen peroxide, which again is involved in the ozone production. The ozone content is most strongly influenced by the values of nitric oxides concentrations  $\text{NO}_x = \text{NO} + \text{NO}_2$ , ozone precursors, mainly  $\text{RO}_2$ , and the solar ultraviolet intensity determining the photodissociation rate. An in-depth minimum in the  $\text{NO}_x$  content during daytime was caused by the photodissociation of  $\text{NO}_2$ .

In these calculations the ozone entrainment flux plays the role of a free parameter: at  $F > F_1$  the ozone concentration value at 24 p.m. will be greater than at 0 a.m., i.e., the increase of ozone concentration takes place, and at  $F < F_1$  – on the contrary – ( $F_1$  is the flux value, for which the calculations were made, Fig. 1). Calculations by the one-box model<sup>25</sup> indicate that the rate of the ozone entrainment flux  $v_0 = F/n(\text{O}_3)$  has a pronounced effect on the final result.

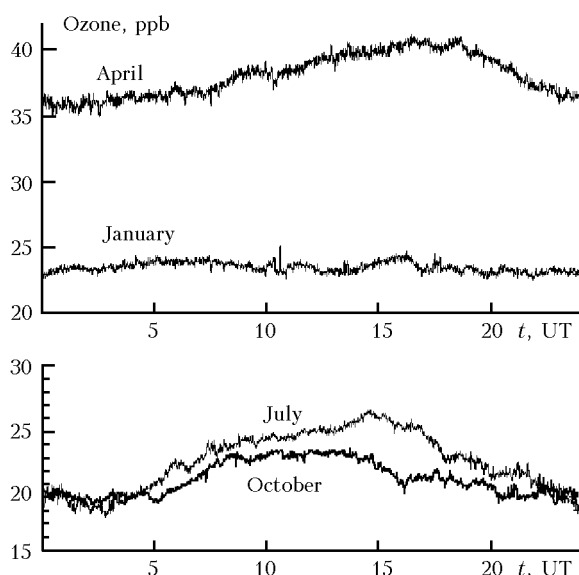


Fig. 2. Daily variations of the ozone concentration for 4 months of 2001 in Lovozero.

The observations revealed that under real conditions the equality of the ozone concentrations at 0 a.m. (night time)  $n_0(\text{O}_3)$  and at 24 p.m.  $n_{24}(\text{O}_3)$ :  $n_0(\text{O}_3) \approx n_{24}(\text{O}_3)$ , averaged over a large time interval, is met highly accurate. Figure 2 shows the diurnal behavior of the ozone concentration during a month of every season in year 2001 based on measurements at the high-latitude geophysical station Lovozero ( $68^\circ\text{N}$ ,  $35.1^\circ\text{E}$ ) located in the Murmansk Region. The averaged data show that the values of ozone concentration at 0 a.m. and 24 p.m. coincide with an accuracy of several tenths of ppb. When we plot the annual behavior of the ozone concentration at this station, the peak value of the mean rate of the

change in concentration is 0.2 ppb/day. Mean values of the ozone concentrations at 0 a.m. and 24 p.m. are close based on the data of different stations. On this basis, we can formulate the balance condition for the diurnal variation of the mean ozone concentration:

$$n_0(\text{O}_3) = n_{24}(\text{O}_3). \quad (2)$$

From this condition and solutions of the equations (1), we can determine the ozone entrainment flux  $F$  corresponding to Eq. (2). In the above example the ozone entrainment flux  $F = F_1$ . The equality (2) enables one to relate the characteristics of the photochemical processes to the characteristics of transfer processes necessary for maintenance of the ozone concentration observed.

The effect of the ozone entrainment flux on the ozone concentration was determined when calculating the dependence of the relative ozone concentration  $[n_{24}(\text{O}_3) - n_0(\text{O}_3)]/n_0(\text{O}_3)$  on the relation  $(F - F_0)/F_0$ , where  $F_0$  is the flux value, at which the equality (2) is performed. The calculations were made for seasonal versions of the characteristics of the north surface atmosphere and the process of interaction of the ozone with the atmosphere given in Table 1. Climatic data in Table 1 are taken from literature<sup>26</sup>; data on the  $\text{NO}_2$  photodissociation are based on the measurements carried out on the Spitsbergen<sup>23</sup>; data on the peak concentration of organic peroxy radicals are based on the simulations of their formation in forest.<sup>17</sup> The results show that the increase (decrease) of the ozone entrainment flux tend to increase (decrease) of ozone concentration during 24 hours. We will point out the influence of the value of the ozone entrainment flux on the relative ozone concentration: the concentration variation, being equal to 1%, is realized when changing the flux by 1 to 2% depending on season. Thus the diurnal variation of the ozone concentration, obtained in model calculations, is a function sensitive of the value of the ozone entrainment flux.

Table 1. Values of the main parameters of the model for the north region

Parameter	Winter	Spring	Summer	Fall
Mean temperature of air, $^\circ\text{N}$	-15	0	15	0
Sunshine duration, hours	2	15	22	9
Peak rate of $\text{NO}_2$ photodissociation, $10^{-3} \text{ s}^{-1}$	0.3	3.6	4.2	1.8
Peak $\text{RO}_2$ concentration, ppb	0.00	0.001	0.02	0.01

The ozone entrainment flux can be found from the solution of Eqs. (1) and (2). The results calculated are presented in Fig. 3, where the flux  $F$  is shown for different seasons: in winter (denoted by W), in spring (S), in summer (Su) and in fall (F). By the season its middle is meant: the middle of January is denoted by W, the middle of April is denoted by S, the middle of July is denoted by Su, the middle of October is denoted by F. The flux

values shown in the figure are connected by lines for a clearer presentation. The calculations were made for the mid-latitude atmosphere (line 1) using the basic parameters, given in Table 2. The initial concentration of nitrogen peroxide  $n_0(\text{NO}_2) = 0.8$  ppb is used as if the  $\text{NO}_x$  content used in calculations exceeds 1 ppb accepted as the boundary between ecologically clean and polluted conditions.<sup>27</sup> Data given in Table 2 correspond to the mean values of the air temperature, sunshine duration, and the rate of  $\text{NO}_2$  photodissociation from Ref. 28 typical of mid-latitudes. The maximum  $\text{RO}_2$  concentration in mid-latitudes is taken twice as large as the concentration used in the calculations for the northern area and shown in Table 1. According to Ref. 9, the height of the mixing layer undergoes significant seasonal variations. The flux  $F$  was found at heights of the mixing layer, being equal to 400 m in winter, 1200 m in spring and autumn, 1500 m – in summer. As follows from Fig. 3, the flux is within  $5 \cdot 10^{10}$ – $1.2 \cdot 10^{11} \text{ cm}^{-2} \cdot \text{s}^{-1}$  for line 1.

**Table 2. Values of main parameters of the model for mid-latitudes**

Parameter	Winter	Spring	Summer	Fall
Mean temperature of air, °N	-10	10	20	10
Sunshine duration, hours	6	14	17	10
Peak daily rate of photodissociation of $\text{NO}_2$ , $10^{-3} \text{ s}^{-1}$	0.6	4.2	6	3.6

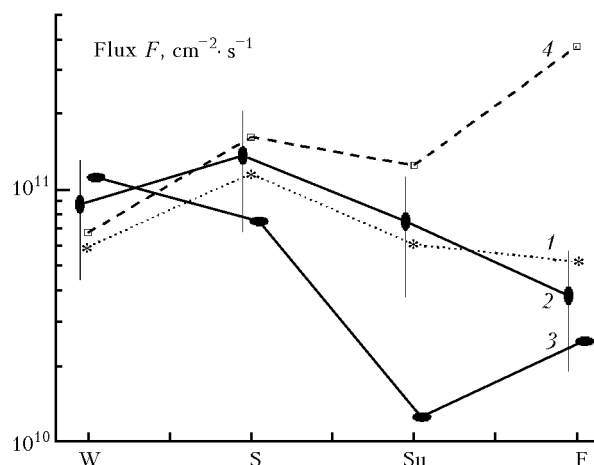


**Fig. 3.** Values of the ozone flux at different heights in the troposphere: (1 and 4) in the upper part of the mixing layer (the calculated results); (2 and 3) at the tropopause (measured results).

Figure 3 shows also the results of processing the experimental data for the latitudes from  $50^\circ$  to  $60^\circ\text{N}$ ,<sup>4</sup> presented with 50% error (line 2), and the results of processing for the latitudes from  $40^\circ$  to  $50^\circ\text{N}$  (line 3). The error for line 3 is the same as for line 2. The results presented by lines 2 and 3 show the mean values of ozone flux in the mid-latitude

troposphere from the stratosphere through the tropopause in different seasons. Thus the values corresponding to the experimental data (lines 2 and 3) give the ozone flux in the upper boundary of the mid-latitude troposphere, and the values, corresponding to line 1, determine the calculated ozone flux at the upper boundary of the mid-latitude mixing layer. Figure 3 shows that the stratospheric ozone flux in the latitude belt from  $50^\circ$  to  $60^\circ\text{N}$  (line 2) is close to the ozone flux to the mid-latitude mixing layer (line 1). The ozone flux on the Earth's surface was measured during summer months and was about  $(1-2) \cdot 10^{11} \text{ cm}^{-2} \cdot \text{s}^{-1}$  in the polar area (Alaska)<sup>5</sup> and was about  $10^{11} \text{ cm}^{-2} \cdot \text{s}^{-1}$  in mid-latitudes (California).<sup>6</sup>

As is seen from the Fig. 3, the ozone flux, described by lines 1 and 2, increases from winter to spring, and then decreases. For a comparison, the ozone entrainment flux is shown by line 4 for conditions of the north (Murmansk) region using the calculated results. These values were obtained based on the data from Table 1 and under the same initial conditions as those in the mid-latitude atmosphere. The results calculated indicate the increase of the ozone flux from winter to fall, in this case the flux is close to the mid-latitude flux from the stratosphere in winter and spring, and it is significantly higher than the mid-latitude flux in summer and in fall. The change of the flux from the value for the mid-latitude atmosphere (line 1) to the value for the high-latitude atmosphere (line 4) in summer and in fall is about 70%, and it is close to the change of the ultraviolet radiation. The remaining 30% are caused by the differences in the concentration of ozone precursors ( $\text{RO}_2$ ) and the atmospheric temperature in mid-latitudes and in high latitudes in these seasons. The stratospheric ozone flux for latitudes from  $40^\circ$  to  $50^\circ\text{N}$  (line 3) decreases from winter to summer, and then increases. Note that a marked decrease of the mid-latitude ozone entrainment flux in summer as compared with the line 1 can be obtained in calculations by increasing the height of the mixing layer (i.e., when decreasing the ozone absorption on the surface), or by increasing the concentration of ozone precursors  $\text{RO}_2$  (i.e., by intensifying the ozone chemical generation).

The results shown in Fig. 3 demonstrate that for maintenance of the ozone concentrations observed in the high-latitude area in summer and in fall in the considered model, higher values of the ozone entrainment flux in the mixing layer are required than in mid-latitudes.

## Conclusion

It is shown that the ozone entrainment flux in the mixing layer can be found from the characteristics of the model describing the ozone behavior in the atmospheric boundary layer. The mean ozone entrainment flux is determined by means of the condition of equality of ozone concentrations

at 0 a.m. and 24 p.m. This condition for the ozone concentration averaged over quite a long time is well fulfilled as the results of observations show. The calculated values of the ozone entrainment flux are in the range from  $5 \cdot 10^{10}$  to  $1.2 \cdot 10^{11} \text{ cm}^{-2} \text{ s}^{-1}$  at the atmospheric parameters accepted and are close to the observed values of the ozone flux coming to the troposphere from the stratosphere in mid-latitudes. It is shown that, for the model considered, the ozone entrainment flux in the mixing layer in high latitudes must exceed the same flux in mid-latitudes.

### Acknowledgments

The work was carried out with the support from the Russian Foundation for Basic Research (grants No. 02-05-64114 and No. 02-05-79148) and INTAS-01-0016.

### References

1. F.Ya. Rovinskii and V.I. Egorov, *Ozone, Nitric and Sulfur Oxides in the Lower Atmosphere* (Gidrometeoizdat, Leningrad, 1986), 183 pp.
2. N.F. Elanskii and O.I. Smirnova, *Izv. Akad. Nauk SSSR, Fiz. Atmos. Okeana* **33**, 597-611 (1997).
3. D.L. Mauzerall, D.J. Jacob, S.-M. Fan, et al., *J. Geophys. Res.* **101**, No. D2, 4175-4188 (1996).
4. A.A. Kukoleva, *Izv. Akad. Nauk SSSR, Fiz. Atmos. Okeana* **38**, No. 1, 95-101 (2002).
5. D.J. Jacob, S.-M. Fan, S.C. Wofsy, et al., *J. Geophys. Res.* **97**, No. D15, 16473-16479 (1992).
6. M.R. Bauer, N.E. Hultman, J.A. Panek, and A.H. Goldstein, *J. Geophys. Res.* **105**, No. D17, 22123-22136 (2000).
7. R.A. Cox, *J. Geophys. Res.* **104**, No. D7, 8047-8056 (1999).
8. S.A. Rumyantsev and V.K. Roldugin, *Ecological Chemistry* **12**, No. 2, 69-78 (2003).
9. B.D. Belan, *Atmos. Oceanic Opt.* **7**, No. 8, 558-562 (1994).
10. J.P. Greenberg, A. Guenter, P. Zimmerman, et al., *Atmos. Environ.* **33**, No. 6, 855-867 (1999).
11. V.K. Roldugin, S.A. Rumyantsev, A.Yu. Karpechko, and M.I. Beloglazov, in: *Kola Peninsula on the Threshold of the Third Thousand Years. Problems of Ecology*, ed. by N.A. Kashulin (KSC, Apatity, 2003), pp. 50-58.
12. J. Crawford, D. Davies, J. Olson, et al., *J. Geophys. Res.* **104**, No. D13, 16255-16273 (1999).
13. R.A. Zavery and L.K. Peters, *J. Geophys. Res.* **104**, No. D23, 30387-30415 (1999).
14. T. Staffelback, A. Neftel, A. Blatter, et al., *J. Geophys. Res.* **102**, No. D19, 23345-23362 (1997).
15. V.A. Isidorov, *Organic Chemistry of the Atmosphere* (Khimizdat, St. Petersburg, 2001), 352 pp.
16. S.M. Semenov, in: *Investigation in the Field of Oceanology, Physics of the Atmosphere, Geography, Ecology, Water Problems and Cryopedology* (GEOS, Moscow, 2001), pp. 173-179.
17. P.A. Makar, J.D. Fuentes, D. Wang, et al., *J. Geophys. Res.* **104**, No. D3, 3581-3603 (1999).
18. A.H. Goldstein, S.C. Wofsy, and C.M. Spivakovsky, *J. Geophys. Res.* **100**, No. D10, 21023-21033 (1995).
19. L. Ganzveld and J. Lellieveld, *J. Geophys. Res.* **100**, No. D10, 20999-21012 (1995).
20. T.A. Markova, "Spatial and temporal variability of ozone concentration in the atmospheric boundary layer," Author's Abstract of Cand. Phys.-Math. Sci. Dissert., Moscow (2002).
21. P. Sander and P.J. Crutzen, *J. Geophys. Res.* **101**, No. D4, 9121-9138 (1996).
22. S. Wunderli and R. Gerig, *Atmos. Environ.* **25A**, 1599-1608 (1991).
23. H. Beine, A. Dahlback, and J.B. Orbak, *J. Geophys. Res.* **104**, No. D13, 16009-16019 (1999).
24. M.A. Lokoshchenko, B.A. Semenchenko, M.A. Kallistratova, and M.S. Pekur, *Atmos. Oceanic Opt.* **7**, No. 7, 522-527 (1994).
25. A.Yu. Karpechko, "Peculiarities of the formation of surface ozone in high latitudes," Author's Abstract of Cand. Phys.-Math. Sci. Dissert., Moscow (2001).
26. B.A. Yakovlev, *Climate of the Murmansk Region* (MKI, Murmansk, 1961), 195 p.
27. J.A. Logan, *J. Geophys. Res.* **88**, No. C15, 10785-10807 (1983).
28. E.E. Berge, H.-C. Huang, J. Chang, and T.-H. Liu, *J. Geophys. Res.* **106**, No. D1, 1347-1363 (2001).